



Dynamic Joint Functional Split and Resource Allocation Optimization in Elastic Optical Fronthaul

Downloaded from: <https://research.chalmers.se>, 2026-04-18 14:13 UTC

Citation for the original published paper (version of record):

Vajd, F., Hadi, M., Bhar, C. et al (2022). Dynamic Joint Functional Split and Resource Allocation Optimization in Elastic Optical Fronthaul. IEEE Transactions on Network and Service Management, 19(4): 4505-4515. <http://dx.doi.org/10.1109/TNSM.2022.3166100>

N.B. When citing this work, cite the original published paper.

© 2022 IEEE. Personal use of this material is permitted. Permission from IEEE must be obtained for all other uses, in any current or future media, including reprinting/republishing this material for advertising or promotional purposes, or reuse of any copyrighted component of this work in other works.

Dynamic Joint Functional Split and Resource Allocation Optimization in Elastic Optical Fronthaul

Faezeh Samimi Vajd, Mohammad Hadi, Chayan Bhar, Mohammad Reza Pakravan, *Member, IEEE*,
and Erik Agrell, *Fellow, IEEE*

Abstract—Dynamic reconfigurability in optical and mobile networks can facilitate heterogeneous service provisioning while utilizing minimal resources. This allows cost-efficient service delivery resulting in high revenues for network operators. Deployment of elastic mobile and optical networks is a key driver for enabling reconfigurability in modern networks. Elastic optical networks can be exploited as the fronthaul portion of new generation of mobile networks. Such elastic optical fronthaul networks facilitate joint reconfiguration of flexible radio and optical elements and provide considerable performance improvements. In this paper, we focus on the joint dynamic selection of functional splits and configuration of optical transponders and illustrate that designing a converged network with optical and radio elements improves network power efficiency. A time-averaged stochastic optimization problem is formulated and its solution is derived using a modified version of the Lyapunov drift technique. Simulation results demonstrate that the proposed scheme can reduce the average power consumption by up to 70% compared to a cloud radio access network with a traditional optical fronthaul. Further, the results show that the modified Lyapunov technique can afford stringent fronthaul delays below 250 μ s. We also discuss how future technology upgrades such as increasing the number of radio antenna ports and decreasing the granularity of fiber spectrum grid may influence the results.

Index Terms—Elastic optical network, fronthaul network, functional split, resource allocation, stochastic optimization.

I. INTRODUCTION

COMMERCIAL deployment of 5G mobile network started in 2019 and continues rapidly worldwide. 5G networks promise high data rates, extensive coverage, and immense connectivity [1]. With these features, 5G can afford diverse and stringent service requirements for extreme mobile broadband communication, mission critical applications, and massive machine-type communication [1], [2].

Early generations of mobile networks had a rigid radio access network (RAN), in which radio and baseband functions were jointly fulfilled in radio units (RUs) installed at cell sites. However, such a rigid structure wastes resources when the RUs work below their capacity [3]. In 4G mobile networks, the so-called cloud-RAN (C-RAN) was introduced, where the baseband functions are performed in a powerful data center named baseband unit pool, and consequently, RUs at cell sites need a simpler and cheaper hardware to only implement radio functions. However, C-RAN suffers from stringent delay and bandwidth requirements on the fronthaul segment, which transfers data samples between RUs and the baseband unit pool [3], [4]. Next-generation radio networks offer a new RAN

architecture, where parts of the baseband functions are still performed at RUs placed in cell sites while the remaining functions are processed at a data center called central unit (CU). A "functional split" determines a demarcation point in the radio protocol stack, before which, the baseband functions are performed locally at the RU, and after which, the functions are processed in the CU [3]. Many functional splits have been proposed by different standardization groups such as third generation partnership project (3GPP) [5], next generation fronthaul interface (NGFI) [6], enhanced common public radio interface (eCPRI) [7], and small cell forum (SCF) [8]. Changing the functional split, the imposed requirements on the fronthaul are mitigated at the cost of more processing in RUs [3]. Efficient selection of functional splits needs a comprehensive view of the network status, which can be provided by software-defined networking (SDN) [9]. The advent of network function virtualization (NFV) enabled flexible functional split selection [3], where various factors such as traffic fluctuation and network conditions may dynamically drive the selection of functional splits [10], [11]. 3GPP introduced an architecture for 5G RAN, which includes two processing points called distribution unit and CU. In this architecture, the conventional fronthaul divides into two sub-networks. The sub-network connecting the RU to the distribution unit is still referred to as fronthaul, while the sub-network between the distribution unit and CU is called midhaul [4]. Here, parts of the baseband processes can be handled in the distribution unit to relieve the processing burden at RUs and CUs [4]. Network slicing is a promising technology that allows operators to further improve resource efficiency of the fronthaul and midhaul networks by allocating resources according to the actual time-varying service requirements [5], [12], [13].

Elastic optical networks (EONs) provide a fine-grained bandwidth allocation by exploiting bandwidth-variable transponders (BVTs) and bandwidth-variable cross-connects (BVXCs). EONs enable reconfiguration of transmission parameters, such as modulation format, coding rate, and number of subcarriers, according to the actual need of time-varying and quality of service (QoS)-dependent traffic demands in contrast to wavelength division multiplexing (WDM) networks, where the network is planned for the peak traffic demands and strictest QoS requirements [14]. EONs increase resource efficiency and consequently, reduce operational expenditures, and offer cost-effective service delivery. A fine-grained EON can be deployed as the fronthaul segment of a RAN to efficiently serve diverse and varying service demands of the mobile network.

In this paper, we propose a dynamic joint flexible functional split selection and resource allocation scheme to reduce power consumption in a RAN served by an elastic optical fronthaul (EOF). Stochastic iterative Lyapunov optimization is employed

F. S. Vajd, M. Hadi, and M. R. Pakravan are with the Department of Electrical Engineering, Sharif University of Technology, Tehran, Iran. E. Agrell is with the Department of Electrical Engineering, Chalmers University of Technology, Gothenburg, Sweden. C. Bhar is with the Department of Electronics and Communication Engineering, National Institute of Technology Warangal, Telangana, India.

to embed average network behavior, instantaneous unexpected conditions, and physical limitations into the scheme to dynamically reconfigure flexible radio and optical elements of the considered EOF-based RAN [15]. A modified version of the Lyapunov technique is proposed to overcome the high queuing delay imposed by the conventional Lyapunov technique while leveraging as much power efficiency as possible from the iterative reconfiguration. Our proposed scheme demonstrates how efficiency is improved by constructive collaboration between radio and optical network operators. Results show that a synergy between optical and radio parts leads to a considerable power saving compared to a traditional C-RAN with fixed optical fronthaul. Further, the performance of the modified Lyapunov is numerically validated by achieving delays below 250 μ s.

The rest of the paper is organized as follows. Some related works are reviewed in Section II. The system model is introduced in Section III. Section IV describes the problem formulation. In Section V, the proposed scheme is evaluated with respect to several reference scenarios. The paper concludes with a discussion in Section VI.

II. RELATED WORKS

Resource allocation in EONs has been an attractive research topic. An impairment aware resource allocation scheme has been presented in [16]; however, the static nature of the formulation cannot support the traffic dynamism of fronthaul networks. Dynamic resource allocation in EONs has been studied in many research works. For instance, [17] proposes a multicast routing and spectrum assignment, which can be used in both dynamic and static contexts. Lyapunov optimization, as a lucrative and versatile tool for dynamic resource allocation in EONs, has been introduced in [15]. Such dynamic schemes do not suit the EON serving as the fronthaul section of a RAN since they do not provide a pervasive abstraction over the whole system to jointly incorporate reconfigurable parameters of the radio and fronthaul networks in the resource allocation process.

As surveyed in [3], the concept of functional splits in RANs is an attractive topic for both industrial and academic societies. The authors of [18] identify some demarcation points in the long-term evolution baseband protocol stack and analyze their associated bandwidth and latency requirements on the fronthaul. They conclude that a proper functional split selection diminishes the fronthaul traffic, which in turn helps to virtualize the required facilities at the CU on general-purpose platforms, and consequently, reduce the total cost. Some researches have concentrated on dynamic reconfiguration of the RAN and flexible functional splitting without a deep consideration of the serving fronthaul network [11], [19], [20].

Due to the interdisciplinary nature of the RANs, optical and radio researchers effectively contribute to the field. A virtual network embedding algorithm is proposed in [21] to flexibly select functional splits for jointly minimizing inter-cell interference and fronthaul bandwidth. It is illustrated that baseband processing centralization can be more beneficial and the fronthaul network can work with less stringent bandwidth and latency requirements if the changes in inter-cell interference level, traffic variation, and distribution of users are efficiently incorporated in the functional split selection. A software-defined integrated framework to optimally select functional splits and allocate bandwidth and wavelength in

a time- and wavelength-division-multiplexing passive optical network (TWDM-PON)-based fronthaul is proposed in [22]. This scheme can increase the bandwidth availability in the fronthaul segment considerably. An end-to-end algorithm is proposed in [23] that jointly optimizes radio resource allocation and functional split selection to maximize throughput while minimizing total deployment cost. The proposed optimization is user-centric and employs SDN and NFV capabilities. An architecture called flexible-RAN (F-RAN) is proposed in [24], which considers inter-cell interference and optical fronthaul resources to efficiently select the appropriate functional split. As reported in [24], the F-RAN reduces wavelength usage while maintaining radio performance at an acceptable level. In [25], a flexible functional split scheme is presented to jointly minimize fronthaul bandwidth and processing power consumption for delay critical applications. In [26], a power-efficient scheme for joint allocation of radio, optical, and mobile edge computing resources in 5G fronthaul is presented; however, the impact of different functional splits on the resource allocation process is not analyzed and only the C-RAN architecture is considered. Although there are some suggestions to establish the fronthaul over an EON [14], [27], [28], no research work has investigated how a fronthaul network can benefit from the flexibility of EONs. Moreover, most of the works do not discuss how technology development influences the performance of their proposed resource allocation schemes.

III. SYSTEM MODEL

We consider the architecture shown in Fig. 1, where I cell sites cover a geographical area. Each cell site has an RU, which is responsible for radio and baseband processing functions (BPFs) and connects to a CU through an EOF. For simplicity, we assume that there is no intermediate distribution unit and midhaul network. The EOF is characterized by an arbitrary topology, whose optical fiber links operate over a spectrum bandwidth consisting of M contiguous frequency slots with bandwidth W [29]. The optical nodes are equipped with BVXCs and BVTs, which provide switch, add, and drop operations for a contiguous batch of frequency slots in an arbitrary spectrum location [14]. We assume that a proper power budgeting guarantees signal-to-noise ratio (SNR) commitments [16], [30]. An SDN controller determines the appropriate functional split for each RU and tunes reconfigurable elements of the EOF in each time interval T . We consider the five functional split options introduced by 3GPP [5] over the uplink path, which is the transmission path from user equipment to the CU, as shown in Fig. 2. Although the downlink path can be included to the model, we only consider the uplink path to simplify description and analysis. The parameters being used in the paper are summarized in Table II.

In the n^{th} time interval, there are $u_i[n]$ users in RU i , each user $j \in \{1, \dots, u_i[n]\}$ sending a traffic load of $l_{i,j}[n]$ b/s to its corresponding RU through the air interface. It is assumed that the functional split of RUs and working bandwidth of BVTs are selected from K different 3GPP functional splits and M equal-bandwidth frequency slots, respectively. Depending on the selected functional split k , parts of the BPFs are performed locally at the RU i to generate a data stream imposing the rate $r_{i,k}[n]$ b/s on the EOF. Assuming an overhead of 6.7% and one sector per RU, the fronthaul rates $r_{i,k}[n]$ are given by

TABLE I: Functional splits and their power, rate, and latency values.

Index	3GPP number [5]	Power consumption (W) [32]	Fronthaul bit rate (Gb/s) [31]	Maximum one-way latency (μ s) [31]
1	2	$p_{i,1}[n] = P_1 + p_{i,2}[n]$	$r_{i,1}[n] = R_1 \sum_{j=1}^{u_i[n]} l_{i,j}[n] + \Gamma_1$	1500 ~ 10000
2	6	$p_{i,2}[n] = P_2 \sum_{j=1}^{u_i[n]} \frac{l_{i,j}[n]}{LY} + p_{i,3}[n]$	$r_{i,2}[n] = R_2 \sum_{j=1}^{u_i[n]} l_{i,j}[n] + \Gamma_2$	250
3	7.2	$p_{i,3}[n] = P_3 \sum_{j=1}^{u_i[n]} \frac{l_{i,j}[n]}{LY} + p_{i,4}[n]$	$r_{i,3}[n] = R_3 \sum_{j=1}^{u_i[n]} l_{i,j}[n] + \Gamma_3$	250
4	7.1	$p_{i,4}[n] = P_4 + p_{i,5}[n]$	$r_{i,4}[n] = R_4 + \Gamma_4$	250
5	8	$p_{i,5}[n] = P_5 + P_6 \sum_{j=1}^{u_i[n]} \frac{l_{i,j}[n]}{LY}$	$r_{i,5}[n] = R_5 + \Gamma_5$	250

TABLE II: List of constants and variables along with their corresponding definitions. Z_a^b denotes the integers $a, a+1, \dots, b$. Two indices referring to the same quantity are distinguished by a prime '.

Type	Notation	Default value	Description
Indices	n, n'	Z_1^N	Interval index
	i, i'	Z_1^I	RU index
	j	$Z_1^{u_i[n]}$	User index
	k	Z_1^K	Split index
	h	Z_0^{K+1}	Power constants index
	Constants	V	1
I		10	Number of RUs
N		200	Number of intervals
K		5	Number of functional splits
T		1 s	Time interval width
M		640	Number of frequency slots
W		6.25 GHz	Frequency slot bandwidth
C		4 b/s/Hz	Modulation spectral efficiency
G		1	Number of guard slots
B		50 GHz	Maximum BVT bandwidth
E		63 W	BVT power bias
F		15.625 W	BVT power slope
η_A		2.3	PUE of RU
η_C		1.1	PUE of CU
η_F		1.2	PUE of BVT
L		375 Mb/s	Maximum RU traffic load per transmission layer
Y		4	Number of transmission layers
Input Parameters	D_0	0.1 Mb	Delay profile constant
	α	2.4 s	Delay profile factor
	ν_0	50 Mb/s	Delay profile shift
	(P_h)	(14,2,5,8,160,30, 40,100,180)	RU power constants
	(R_k)	(1.067,1.067,7.6483, 11.4724,20.9781)	EOF bit rate constants
	(Γ_k)	(0.0256,1.4084,0.128, 0.0854,0)	Uplink radio overhead
	$(Q_{i,i'})$	Z_0^1	Intersecting shortest paths
	$\mathbf{u}[n] = (u_i[n])$	\sim Poisson	Number of users per RU
	$\mathbf{L}[n] = (l_{i,j}[n])$	\sim Lognormal	User load
	Output Parameters	$p[n]$	$[0, \infty)$
$\mathbf{q}[n] = (q_i[n])$		Z_0^∞	Actual queue backlog
$\mathbf{a}[n] = (a_i[n])$		Z_0^∞	Arrived bits to fronthaul
$\mathbf{s}[n] = (s_i[n])$		Z_0^∞	Served bits by fronthaul
$\mathbf{h}[n] = (h_i[n])$		Z_1^{640}	Start frequency slot
$\mathbf{b}[n] = (b_i[n])$		Z_0^8	Servicing frequency slots
$\mathbf{t}[n] = (t_{i,i'}[n])$		Z_0^1	Relative spectrum location
$\mathbf{x}[n] = (x_{i,k}[n])$		Z_0^1	Selected functional split
$\mathbf{y}[n] = (y_i[n])$		Z_0^1	BVT activation

power efficiency. To this end, the conventional Lyapunov technique, as a versatile dynamic stochastic optimization method, is presented. Then, we describe the optimization problem and propose an efficient way based on a modified version of the Lyapunov technique to solve it.

A. Lyapunov technique

The Lyapunov drift plus penalty algorithm, or shortly called Lyapunov algorithm, is an efficient technique for stochastic minimization of a time-averaged objective function in a large-

scale system subject to a set of time-averaged and non-time-averaged constraints. Queue stability commitments are common examples of time-averaged constraints [35].

Assume that we have a large system (e.g., the EOF described in Section III) and let the time be split into consecutive time intervals. The system is described by its stochastic time-varying state (e.g., user traffic) in every interval. In each interval, depending on the state of the system, a proper action (e.g., transponder configuration) should be taken to prepare the system to react to the system state change. The optimum action is the solution of a large-scale stochastic optimization problem subject to a set of time-averaged and non-time-averaged constraints. Generally, the optimum action in a given interval depends on the status of the system in previous and future intervals. Such dependencies are described by time-averaged constraints. Time-averaged constraints make the decision on the actions non-causal and very complicated. This is where the Lyapunov technique comes to play and allows to decompose the complex decision process into a sequence of causal and simple sub-processes, each determining the proper action of an interval based on the state information of the current and previous intervals.

As shown in the flowchart of Fig. 3, after ‘‘initialization’’ of some state variables (e.g., transponder queue lengths), in each interval, a sequence of processes run. The optional ‘‘delay control’’ step is our proposed modification of the conventional Lyapunov formulation, to be discussed below. In the ‘‘decision’’ step, an instantaneous optimization including all instantaneous constraints of the original problem but no time-averaged constraints is solved. The objective function of the instantaneous optimization is a summation of two terms, one representing the objective of the original problem weighted by a factor called ‘‘Lyapunov penalty coefficient’’, and the other is a drift penalty term related to the time-averaged constraints of the original problem. State variables are included in the drift penalty term and can prioritize the minimization of the penalty term over the objective term in some intervals. After solving the instantaneous optimization, the proper ‘‘action’’ is determined and the system is retuned accordingly. Finally, in the ‘‘update’’ state, the values of the state variables are renewed by some recursive expressions involving the current and previous states of the system as well as the taken action. The interaction of the recursive update expressions and drift penalty term holds the time-averaged constraints of the original problem satisfied.

An important drawback of the conventional Lyapunov technique is its slow response in scenarios with strict delay constraints. Although the conventional Lyapunov method eventually satisfies the required time-averaged values, the instantaneous delay values may be far away from their corresponding time-averaged values in some intervals resulting in unacceptably high jitter (i.e., delay variance). To relieve this issue, we introduce the block labeled ‘‘delay control’’ in

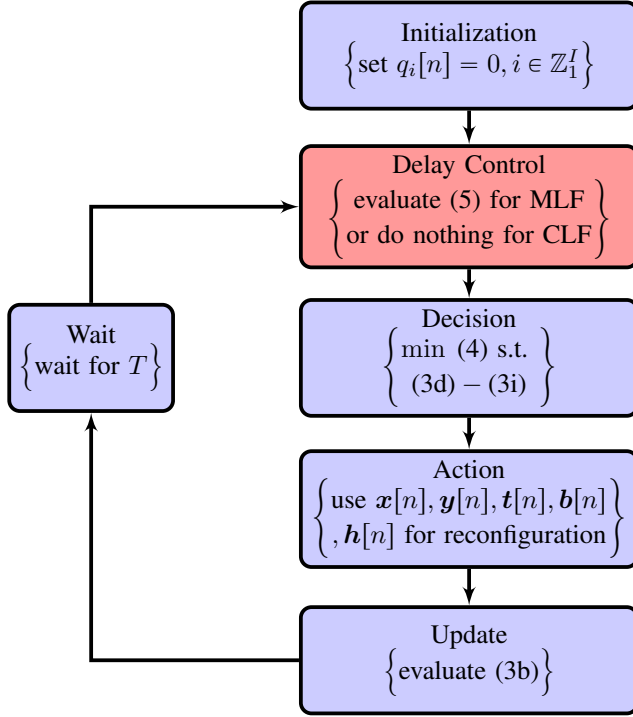


Fig. 3: Flowchart of the Lyapunov optimization. CLF and MLF stand for conventional Lyapunov formulation and modified Lyapunov formulation, respectively. Only the “Delay Control” step is different for CLF and MLF. For some pre-defined assumptions, the convergence of CLF is mathematically proven [35]. The equations and notations involved in each step of the MLF are given in braces { }.

Fig. 3.

Under some special conditions, the convergence of the Lyapunov method to the optimum solution of the problem is mathematically guaranteed [35]. This is not the case in general, but the performance of the Lyapunov method can nevertheless be near optimum in practical applications [36].

B. Proposed optimization process

Considering the described system model in Section III, we require an optimization that uses the network topology, number of users $u_i[n]$, and traffic of users $l_{i,j}[n]$ as the input, and determines functional split and configuration of BVTs as the output such that the total time-averaged power consumption is minimized while physical constraints are satisfied. Generally, the optimization has a complex structure beyond the capabilities of the available software optimizers. To address this issue, we use a modified version of the Lyapunov tool to decompose the optimization into several simple, affordable, and interconnected sub-optimizations.

The optimization includes binary variables $x_{i,k}[n]$, $y_i[n]$, and $t_{i,i'}[n]$, and nonnegative integer variables $h_i[n]$ and $b_i[n]$, where the range of indices is given in Table II. $x_{i,k}[n]$ is 1 if RU i uses functional split k in interval n and 0 otherwise, while $y_i[n]$ equals 1 if the BVT of RU i is active in interval n and 0 otherwise. $t_{i,i'}[n]$ takes the value of 1 in interval n for $h_i[n] \leq h_{i'}[n]$ and 0 otherwise. The total power consumption in interval n is

$$\begin{aligned}
 p[n] = & \sum_{i=1}^I [\eta_F b_i[n](E + FC) + \\
 & \eta_A \sum_{k=1}^K x_{i,k}[n] p_{i,k}[n] + \\
 & \eta_C \sum_{k=1}^K x_{i,k}[n] (P_0 + p_{i,1}[n] - p_{i,k}[n])], \quad (1)
 \end{aligned}$$

which sums the power consumption of transponders, RUs, and CU as the main sources of the traffic-dependent power consumption. Depending on the selected functional split, $a_i[n]$ bits arrive to the queue i in interval n , and $s_i[n]$ bits are served according to (2a) and (2b), respectively.

$$a_i[n] = T \sum_{k=1}^K x_{i,k}[n] r_{i,k}[n], \quad i \in \mathbb{Z}_1^I, \quad (2a)$$

$$s_i[n] = TWCb_i[n], \quad i \in \mathbb{Z}_1^I. \quad (2b)$$

Ideally, if the number of users in RUs $\mathbf{u}[n]$ and user traffic demands $\mathbf{L}[n]$ were known in advance for a sequence of intervals $n = 1, 2, \dots, N$, then the whole block of resources could be optimized jointly via the noncausal formulation

$$\min_{\mathbf{x}[n], \mathbf{y}[n], \mathbf{t}[n], \mathbf{b}[n], \mathbf{h}[n], n \in \mathbb{Z}_1^N} \bar{p} = \frac{1}{N} \sum_{n=1}^N \mathcal{E}\{p[n]\} \quad \text{s.t.} \quad (3a)$$

$$q_i[n+1] = \max\{q_i[n] + a_i[n] - s_i[n], 0\}, \quad i \in \mathbb{Z}_1^I, \quad (3b)$$

$$\bar{a}_i \leq \bar{s}_i, \quad i \in \mathbb{Z}_1^I, \quad (3c)$$

$$h_i[n] + b_i[n] \leq M, \quad i \in \mathbb{Z}_1^I, \quad (3d)$$

$$a_i[n] - s_i[n] \leq D_i, \quad i \in \mathbb{Z}_1^I, \quad (3e)$$

$$\sum_{k=1}^K x_{i,k}[n] = 1, \quad i \in \mathbb{Z}_1^I, \quad (3f)$$

$$Wb_i[n] \leq By_i[n], \quad i \in \mathbb{Z}_1^I, \quad (3g)$$

$$t_{i,i'}[n] + t_{i',i}[n] = 1, \quad i, i' \in \mathbb{Z}_1^I : i \neq i', \quad (3h)$$

$$h_i[n] + b_i[n] + G \leq h_{i'}[n] + M(4 - t_{i,i'}[n] - y_i[n] - y_{i'}[n] - Q_{i,i'}), \quad i, i' \in \mathbb{Z}_1^I : i \neq i'. \quad (3i)$$

The objective function \bar{p} in (3a) is the time-averaged total power consumption with an expectation over the random variables $u_i[n]$ and $l_{i,j}[n]$ [35]. The queue backlog is recursively updated by (3b). Queue stability is ensured by constraint (3c), where the average service rate of each queue is held equal to or larger than the corresponding average arrival rate [35]. The same expression as \bar{p} is used to calculate \bar{a}_i and \bar{s}_i in (3c). The assigned slots are kept within the fiber bandwidth by (3d). To meet the stringent latency requirements of the fronthaul, (3e) holds the number of stored bits $a_i[n] - s_i[n]$ of queue i in each interval n below D_i . Each RU chooses exactly one functional split by (3f). As constrained by (3g), no frequency slot is occupied if the BVT of RU i is inactive in interval n , i.e., $y_i[n] = 0$, while if the BVT is active, i.e., $y_i[n] = 1$, the occupied bandwidth cannot be larger than B . The relative locations of the frequency slots assigned to every pair of BVTs are given by (3h). Constraint (3i) places a minimum of G guard frequency slots between the frequency slots allocated to BVTs of RUs i and i' with intersecting shortest paths $Q_{i,i'} = 1$ having at least one common link. It is worth noting that (3) is quite general and versatile and can include more constraints on routing, capacity, SNR, QoS, network slicing and so on. For example, routing requirements can be included to the formulation as described in [37].

In addition to the huge number of constraints and variables proportional to N , the noncausal structure impedes the constructed optimization (3) to be practically deployed. Fortunately, with the Lyapunov technique described in Subsection IV-A, the formulation can be approximated by a causal sequence of simple sub-optimization problems, which are interconnected by some recursive update equations. Adopting

the Lyapunov technique, in each interval n , the SDN controller solves an optimization problem with the constraints (3d)–(3i) and the objective

$$\min_{\substack{\mathbf{x}[n], \mathbf{y}[n], \mathbf{t}[n] \\ \mathbf{b}[n], \mathbf{h}[n]}} Vp[n] + \sum_{i=1}^I q_i[n](a_i[n] - s_i[n]). \quad (4)$$

After solving (4), the queue lengths are updated according to (3b) with the initialization $q_i[1] = 0, i \in \mathbb{Z}_1^I$. Due to the existence of the queue-dependent constraint (3e), this step-by-step optimization deviates from the tight conditions required for mathematical proof of the convergence [35]. However, as demonstrated numerically in [36], it still approaches the time-averaged total power consumption \bar{p} in many practical scenarios with a proximity controlled by the so-called Lyapunov coefficient V . The interaction of the penalty term in (4) and the update equation (3b) ensures the constraint (3c) and consequently, the queue stability [35].

Unfortunately, the conventional Lyapunov technique cannot afford stringent latency requirements, which are commonly required for the EOF. To address this issue, we added the constraint (3e) to the formulation. To further control latency requirements, D_i in constraint (3e) can be selected according to the known status parameters such as average data rate of the i^{th} RU $\nu_i = \frac{1}{N} \sum_{n=1}^N \sum_{j=1}^{u_i[n]} l_{i,j}[n]$. An applicable relationship can be

$$D_i = D_0 + \alpha \max\{\nu_i - \nu_0, 0\}, \quad i \in \mathbb{Z}_1^I, \quad (5)$$

where D_0 , α , and ν_0 are constants. Using the conventional Lyapunov technique, the arrived bits accumulate in the queue until the backlog makes the penalty term of (4) dominant. Then, the optimization has to serve the queue to reduce the penalty term. If the data rate and equivalently, the arrival rate is low, the penalty term takes too long to become dominant, which in turn leads to unacceptable delays. This is where the equation (5) comes into play and tightens D_i in constraint (3e) to accelerate the queue serving even when the penalty term is not sufficiently dominant. On the other hand, D_i takes higher values by (5) when the data rate increases. This loosens the constraint (3e) and improves the power efficiency by avoiding hasty queue serving. For the high data rate, the fast growth of the queue backlog makes the penalty term dominant and forces the queue backlog to be served within an acceptable latency.

Ignoring the described modifications of the latency control mechanism in (3e) and (5), the proposed formulation is a customized version of the conventional Lyapunov technique, as emphasized on using the equations and notations given in each step of the flowchart in Fig. 3. The latency control mechanism is included in the flowchart as a red block, where nothing is done if the conventional Lyapunov is used.

V. NUMERICAL RESULTS

The performance of the proposed scheme, i.e., the objective function (4) constrained to (3d)–(3i), is evaluated over the network topology of Fig. 1, where $I = 10$ RUs (hexagonal nodes) are connected to a CU (square node). The network topology is adapted from a real network covering the Stockholm area [36]. The link propagation delay is assumed to be $5 \mu\text{s}/\text{km}$. The number of users in each RU is extracted from a Poisson distribution with a mean of ρ . The traffic loads of

users are independent and identically distributed with a log-normal distribution that has mean μ and standard deviation σ in each interval. Clearly, the total traffic load of each RU has a compound Poisson distribution with the mean $\nu = \rho\mu$ and standard deviation $\sqrt{\rho} \exp(\mu + \sigma^2)$ [38]. The coefficient of variation (CV), which is the ratio of the standard deviation to the mean, is used as an indicator of the traffic variation in each RU. We change ρ to produce various average traffic loads ν while CV is kept at a desired value by tuning μ and σ for each traffic load. By default, $\text{CV} = 2$ [36] when the average traffic is swept. For fixed values of μ and ρ , the standard deviation σ is changed to generate different values of CV at a fixed average traffic load ν . For air interface bandwidth of 100 MHz, sampling frequency of 153.6 MHz, 4 antenna ports, $Y = 4$ transmission layers, no channel coding, 64 quadrature amplitude modulation (QAM), and sample bitwidth of 16, L , R_k , and P_h equal to the given default values in Table II, where the default values of the other parameters are also available. The considered air interface configuration provides a maximum acceptable uplink traffic load of $L = 375 \text{ Mb/s}$ per each transmission layer in RU [31]. We set $D_0 = 0.1 \text{ Mb}$, $\alpha = 2.4 \text{ s}$, and $\nu_0 = 50 \text{ Mb/s}$ in the profile (5) to keep the queuing delay below a few microseconds and hence, maintain the overall latency of the fronthaul, including the propagation delay, below $250 \mu\text{s}$ to satisfy the most stringent latency required for the considered functional splits in Table I [31]. The average queuing delay is computed by means of Little's theorem [35]. The shortest paths from each RU to the CU is pre-computed for the considered network topology and then, the intersecting shortest paths $Q_{i,i'}$ are determined by finding the shortest paths with at least one common link. YALMIP is used to model the optimization problem in MATLAB while CPLEX is employed to numerically solve the modeled optimization over $N = 200$ intervals of $T = 1 \text{ s}$. Simulations run on a desktop computer with a Corei5-4200U processor, and 4 GB installed physical memory, where solving the optimization problem in each iteration takes around 44 ms.

Due to the existence of the queue-dependent constraint (3e), the convergence of the proposed formulation is not mathematically proven. However, as illustrated in Fig. 4, the convergence can be numerically validated for our simulation scenarios. This numerical validation is in accordance with the claims in [36] on the general performance of the Lyapunov method. In Fig. 4, averaged values of the transponders, RUs, CU, and total power consumption versus the number of intervals N are plotted. To be more precise, for each N , the power consumption values are averaged from over intervals $1, 2, \dots, N$. Clearly, after an initial transient, the power curves converge to a constant value validating the expected convergence. The figure also shows how different sources of power consumption contribute to the total power consumption for the assumed default values of Table II. It is worth noting that increasing the number of intervals N beyond 200 has almost no effect on the converged values. Thus, $N = 200$ was selected for the simulations in this paper.

Employing centralized functional splits imposes higher data rates on the fronthaul and consequently, the EOF consumes much power, while the power consumption of BPFs reduces due to centralization in the CU. In contrast, by using less-centralized functional splits, lower data rates are required on the fronthaul, which in turn decreases the consumed power in the EOF. However, the power consumption of BPFs increases because they are implemented at RUs with a high PUE.

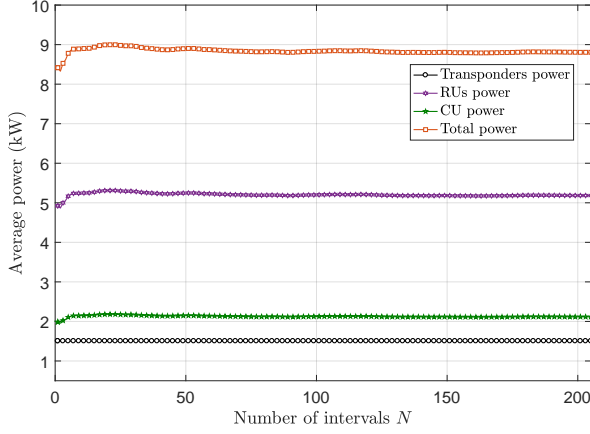


Fig. 4: Averaged values of transponders, RUs, CU, and total power consumption versus number of intervals N .

Therefore, there is a tradeoff between power consumption of the EOF and BPFs, which is dynamically controlled by the chosen functional split. In the proposed scheme, the functional split type and EOF configuration can be flexibly changed to exploit this applicable tradeoff for minimizing the total power consumption. The power saving of the proposed dynamic scheme is compared to that of a semi-rigid counterpart scheme, where the EOF is flexibly reconfigured while the functional split is permanently fixed. The power saving of a scheme is defined as the relative power consumption of that scheme with respect to the power consumption of a reference rigid scheme, where a traditional C-RAN with 50-GHz WDM fronthaul is employed [39]–[41]. Clearly, in the rigid scheme, no reconfiguration is carried out to adapt network configuration to the traffic changes. The rigid scheme coincides with the architecture commercially implemented by many 4G/5G mobile operators [42]. As a result, it is a suitable reference benchmark for the proposed dynamic scheme. In fact, our simulation results show how flexibility in functional split selection and configuration of EOF reduces power consumption. Such results can help operators to more efficiently plan their development and investment directions.

Fig. 5 reports the power savings of the proposed dynamic scheme and its semi-rigid counterparts versus average RU traffic ν . For all the schemes, a considerable amount of power saving, up to around 70%, compared to the rigid scheme is observed. This notable saving originates from the flexibility of the EOF, which allows to allocate resources according to the actual needs, unlike the rigid scheme, where the resources are allocated beyond the actual time-varying needs. Further, for all the schemes, the power saving declines by increasing the traffic load since more processing power is required to handle higher traffic loads. Fixing the functional split in the semi-rigid schemes can reduce the power-saving. For example, if the semi-rigid scheme is forced to use the first functional split, the power saving decreases by 5–11 percentage points (p.p.) compared to the dynamic scheme. In fact, a flexible selection of functional splits in the dynamic scheme leads to more power-efficient resource allocation. Among the semi-rigid schemes, a fixed selection of the fifth functional split provides almost the same power saving as the dynamic scheme; however, such an observation is not always true for other scenarios,

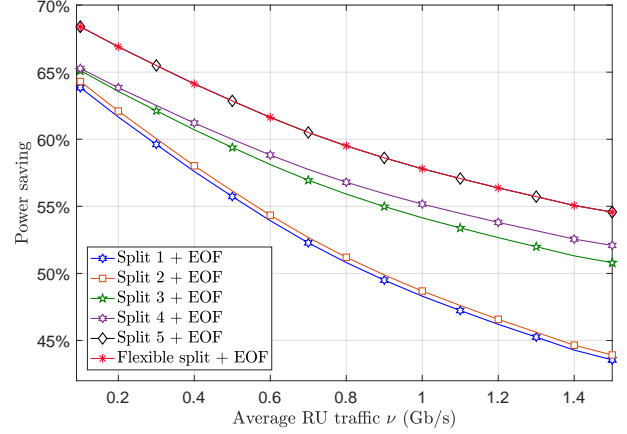


Fig. 5: Power saving compared to the rigid scheme versus average RU traffic for dynamic and semi-rigid schemes.

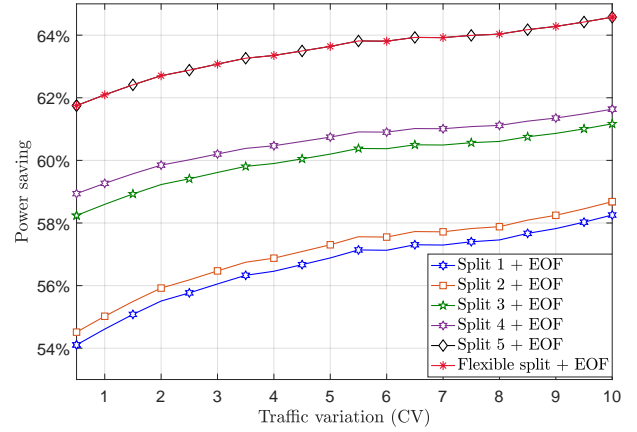


Fig. 6: Power saving compared to the rigid scheme versus RU traffic variation for dynamic and semi-rigid schemes.

as discussed later. The power saving of the schemes versus RU traffic variation is plotted in Fig. 6, where RUs are loaded by a third of the full traffic capacity YL . The curves stand in the same order as in Fig. 5. The power saving improves by at most 3 p.p. as the traffic variation increases. This small improvement arises from the fact that the impact of flexibility is more evident when the traffic fluctuates more.

Technology evolves rapidly in all parts of a future RAN architecture, including EOF, RU, and CU. Analyzing the performance of the proposed scheme while encountering new technologies is noticeable. Fig. 7 shows how power saving of the proposed dynamic scheme changes as the technology grows in various aspects. The red curve corresponds to the conventional technology situation, whose parameters are given while describing the simulation setup. Reducing the spectrum granularity of the EOF is a technology trend, which allows to more efficiently utilize spectrum resources, and consequently reduce power consumption. As shown by the purple curve in Fig. 7, reducing the spectrum granularity W from 6.25 GHz to 3.125 GHz improves the power saving by 2 p.p. compared to the considered conventional situation. For the spectrum granularity of 3.125 GHz, functional split 4 is the dominant selection. This is where the importance of the flexibility in functional split selection appears. Assume that we use a semi-rigid scheme that forces the selection of the functional split 5. If the EOF is upgraded to a finer spectrum granularity,

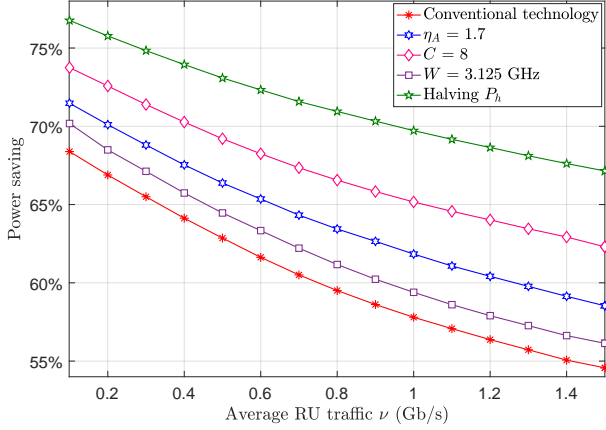


Fig. 7: Power saving of the dynamic scheme versus average RU traffic (Gb/s) for various technology trends.

the functional split 5 is no longer the best choice. So, if the selection of the functional split is not flexible, the maximum possible power saving is not achieved. If the efficiency of the maintenance facilities at RUs increases such that $\eta_A = 1.7$, functional split 5 is dominantly selected by the dynamic scheme and up to 4 p.p. more power saving is obtained, as shown by the blue curve of Fig. 7. The pink curve in the figure shows that power saving increases to 74% when BVTs employ a higher order modulation format such as dual-polarization 16-QAM with a spectral efficiency of $C = 8$ b/s/Hz. When the modulation spectral efficiency increases, the high-traffic functional split 5 is selected frequently because BVTs with high-order modulation formats afford the imposed fronthaul rate with a lower number of allocated frequency slots and consequently, a lower power consumption. As the green curve of Fig. 7 shows, doubling the baseband processing capability or equivalently, halving P_h , provides a considerable power saving, up to 12 p.p. more than the conventional technology situation. Again, the functional split 5 is dominantly selected but now, the required baseband power consumption is halved as a result of doubling the processing capability.

Future 5G networks have to support high data rates and consequently, the capacity of cells should be enhanced. This can be achieved by adding more antenna ports in RUs and increasing number of transmission layers Y or by using wider radio bandwidths by employing more carriers. Furthermore, to reduce the power consumption of BPFs, power-efficient digital hardware should be used. We, therefore, consider a hypothetical future 5G network with $W = 3.125$ GHz and $Y = 8$, where the number of antenna ports is increased to 8 and P_h is halved. As evident from Fig. 9, functional splits 3 and 4 are now selected in the dynamic scheme. This leads to 70% and 45% power savings under low and high traffic conditions, respectively, as can be seen in Fig. 8. Increasing the number of antenna ports, split 5 needs wider bandwidth on the EOF and therefore, the power consumption of the BVT increases. In contrast, the power dissipation for BPFs at RUs in splits 1 and 2 increases on increasing the number of transmission layers and the number of antenna ports. Here, splits 3 and 4 have a moderate behavior in terms of the power consumed at RU and EOF and are selected frequently by the dynamic scheme, as shown in Fig. 9. As a notable observation in Fig. 8, the semi-rigid scheme with functional split 5 performs 10 p.p. worse than the dynamic scheme. This

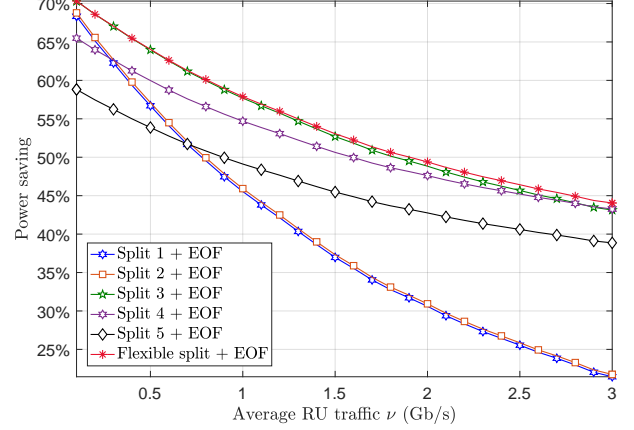


Fig. 8: Power saving versus average RU traffic in a hypothetical scenario, where technology upgrades change Y , W , P_h , and number of antenna ports.

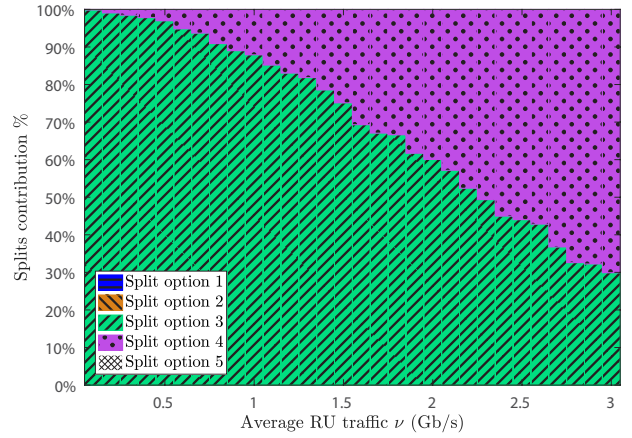


Fig. 9: Functional split contribution of the dynamic scheme versus average RU traffic in a hypothetical scenario, where technology upgrades change Y , W , P_h , and number of antenna ports.

again signifies the importance of flexibility in functional split selection as technology changes or upgrades. If the selection of the functional split 5 is inherited from the conventional technology situation, an undesired 10 p.p. drop in the power saving is compelled. The importance of flexibility is doubled in self-organising networks, where the involved parameters such as bandwidth, number of antenna ports, and number of transmission layers may be dynamically changed. Moreover, it is observed that up to the average traffic load of 80 Mb/s, functional splits 1 and 2 outperform functional split 5 due to their lower bandwidth requirements, which can be fully served by allocating only one 3.125-GHz frequency slot. As the average RU traffic increases in Fig. 9, functional split 4 is used more since it requires fewer BPFs at the RUs and benefits more from centralization.

Fig. 10 represents the power saving versus RU traffic variation for an average traffic of $\nu = 1$ Gb/s. The power saving increases by up to 4 p.p. as traffic varies more around its mean. Here, the proposed dynamic scheme achieves a 10 p.p. improvement in power saving compared to the semi-rigid scheme with functional split 5, which is the best semi-rigid scheme in Fig. 6. Functional splits 3 and 4 contribute 90% and 10%, almost independently of the traffic variation, to the functional split selection, as shown in Fig. 11.

In all the simulation scenarios, the EOF latency is less

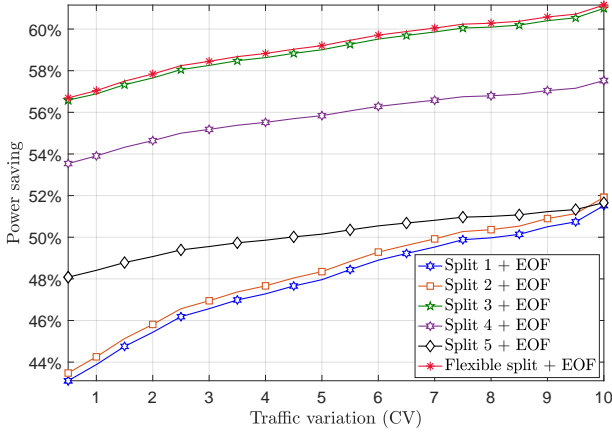


Fig. 10: Power Saving versus RU traffic variation in a hypothetical scenario, where technology upgrades change Y , W , P_h , and number of antenna ports.

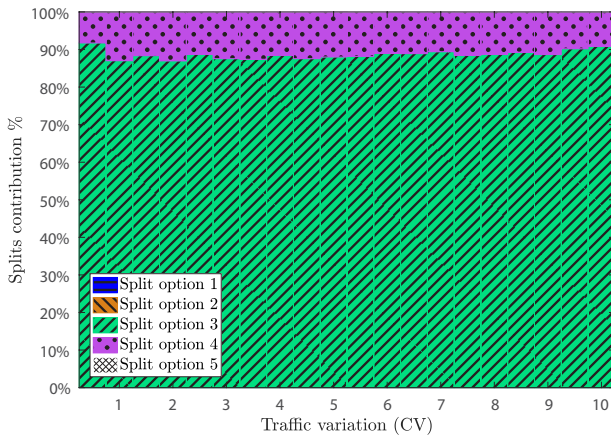


Fig. 11: Functional split contribution of the dynamic scheme versus RU traffic variation in a hypothetical scenario, where technology upgrades change Y , W , P_h , and number of antenna ports.

than $250 \mu\text{s}$ which indicates the capability of the modified Lyapunov technique in controlling delay. Undoubtedly, the reported improvement values should be considered as an upper bound on the practical improvement values for the real deployment of the proposed formulation. The practical improvement gets closer to its corresponding reported upper bound at the cost of considering a more sophisticated description of the system model and as a result, including more detailed constraints into the formulation. Since the most important constraints are already included in the proposed formulation, we expect that the gap between the reported and practical improvement values is negligible.

VI. CONCLUSION

This paper presents a framework that jointly optimizes functional split selection and resource allocation in a RAN with EOF. The framework aims to minimize total power consumption while satisfying physical limitations. We modify the traditional Lyapunov optimization technique such that the stringent latency requirements of the EOF are satisfied. The modified Lyapunov technique numerically solves the complex optimization problem of joint functional split selection and resource allocation in a chain of interconnected simple optimizations, while ensuring an extremely low queuing delay. Results show that the proposed scheme reduces the average

power consumption, including the power consumed by BPFs and transponders, by 50%–70% compared to a conventional C-RAN with WDM fronthaul. The obtained power saving arises from the inherent flexibility of the scheme in EOF configuration and functional split selection. In fact, in the EOF, the resources are allocated according to the actual traffic demands, unlike the conventional WDM fronthaul, where the resources are over-provisioned for the worst traffic conditions. The flexible functional split selection also compromises the rate requirements imposed on the EOF against the power-efficient centralized processing of BPFs in the CU. We also demonstrate how flexibility in functional split selection and EOF reconfiguration helps to improve power efficiency under the expected future technology upgrades. A flexible adaptation of the functional split to the upgraded network elements brings up to 10 p.p. more power efficiency compared to a counterpart scheme, whose functional split is fixed. The generality and versatility of the proposed scheme allow to incorporate into the problem a more detailed description of the QoS and physical constraints over a more realistic system model. This can be an interesting topic of future research.

REFERENCES

- [1] A. A. Zaidi, R. Baldemair, H. Tullberg, H. Borgegren, L. Sundstrom, J. Medbo, C. Kilinc, and I. Da Silva, "Waveform and numerology to support 5G services and requirements," *IEEE Communications Magazine*, vol. 54, no. 11, pp. 90–98, 2016.
- [2] C.-X. Wang, F. Haider, X. Gao, X.-H. You, Y. Yang, D. Yuan, H. M. Aggoune, H. Haas, S. Fletcher, and E. Hepsaydir, "Cellular architecture and key technologies for 5G wireless communication networks," *IEEE communications magazine*, vol. 52, no. 2, pp. 122–130, 2014.
- [3] L. M. Larsen, A. Checko, and H. L. Christiansen, "A survey of the functional splits proposed for 5G mobile crosshaul networks," *IEEE Communications Surveys & Tutorials*, vol. 21, no. 1, pp. 146–172, 2018.
- [4] I. GSTR-TN5G, "Transport network support of IMT-2020/5G," 2018.
- [5] 3GPP, "3GPP TR 38.801 V14.0.0 (2017-03): Study on new radio access technology: Radio access architecture and interfaces." 3GPP, 2017.
- [6] IEEE 1914 website, "https://sagroups.ieee.org/1914/."
- [7] "eCPRI Specification V1.1 Common Public Radio Interface: eCPRI Interface Specification."
- [8] Small Cell Forum, "Solving the HetNet puzzle Small cell virtualization functional splits and use cases."
- [9] E. J. Kitindi, S. Fu, Y. Jia, A. Kabir, and Y. Wang, "Wireless network virtualization with SDN and C-RAN for 5G networks: Requirements, opportunities, and challenges," *IEEE Access*, vol. 5, pp. 19099–19115, 2017.
- [10] S. Matoussi, I. Fajjari, S. Costanzo, N. Aitsaadi, and R. Langar, "5G RAN: Functional split orchestration optimization," *IEEE Journal on Selected Areas in Communications*, vol. 38, no. 7, pp. 1448–1463, 2020.
- [11] A. M. Alba and W. Kellerer, "A dynamic functional split in 5G radio access networks," in *IEEE Global Communications Conference (GLOBECOM)*. IEEE, 2019.
- [12] I. Afolabi, T. Taleb, K. Samdanis, A. Ksentini, and H. Flinck, "Network slicing and softwarization: A survey on principles, enabling technologies, and solutions," *IEEE Communications Surveys & Tutorials*, vol. 20, no. 3, pp. 2429–2453, 2018.
- [13] J. V. Ramrao and A. Jain, "Dynamic 5G network slicing," *International Journal of Advanced Trends in Computer Science and Engineering*, vol. 10, no. 2, 2021.
- [14] R. Boutaba, N. Shahriar, and S. Fathi, "Elastic optical networking for 5G transport," *Journal of Network and Systems Management*, vol. 25, no. 4, pp. 819–847, 2017.
- [15] M. Hadi and E. Agrell, "Iterative configuration in elastic optical networks," in *International Conference on Optical Network Design and Modeling (ONDM)*. IEEE, 2020.
- [16] L. Yan, E. Agrell, H. Wymeersch, and M. Brandt-Pearce, "Resource allocation for flexible-grid optical networks with nonlinear channel model [invited]," *Journal of Optical Communications and Networking*, vol. 7, no. 11, pp. B101–B108, 2015.
- [17] M. Moharrami, A. Fallahpour, H. Beyranvand, and J. A. Salehi, "Resource allocation and multicast routing in elastic optical networks," *IEEE Transactions on Communications*, vol. 65, no. 5, pp. 2101–2113, 2017.
- [18] U. Dötsch, M. Doll, H.-P. Mayer, F. Schaich, J. Segel, and P. Sehier, "Quantitative analysis of split base station processing and determination of advantageous architectures for LTE," *Bell Labs Technical Journal*, vol. 18, no. 1, pp. 105–128, 2013.

- [19] S. Matoussi, I. Fajjari, S. Costanzo, N. Aitsaadi, and R. Langar, "A user centric virtual network function orchestration for agile 5G cloud-RAN," in *IEEE International Conference on Communications (ICC)*. IEEE, 2018.
- [20] H. Mei and L. Peng, "Flexible functional split for cost-efficient C-RAN," *Computer Communications*, vol. 161, pp. 368–374, 2020.
- [21] D. Harutyunyan and R. Riggio, "Flex5G: Flexible functional split in 5G networks," *IEEE Transactions on Network and Service Management*, vol. 15, no. 3, pp. 961–975, 2018.
- [22] A. Marotta, D. Cassioli, K. Kondepu, C. Antonelli, and L. Valcarenghi, "Efficient management of flexible functional split through software defined 5G converged access," in *IEEE International Conference on Communications (ICC)*, 2018.
- [23] S. Matoussi, I. Fajjari, N. Aitsaadi, R. Langar, and S. Costanzo, "Joint functional split and resource allocation in 5G Cloud-RAN," in *IEEE International Conference on Communications (ICC)*, 2019.
- [24] Y. Li, J. Mårtensson, B. Skubic, Y. Zhao, J. Zhang, L. Wosinska, and P. Monti, "Flexible RAN: combining dynamic baseband split selection and reconfigurable optical transport to optimize RAN performance," *IEEE Network*, 2020.
- [25] M. Tohidi, H. Bakhshi, and S. Parsaeefard, "Flexible function splitting and resource allocation in C-RAN for delay critical applications," *IEEE Access*, vol. 8, pp. 26 150–26 161, 2020.
- [26] T. Lagkas, D. Klonidis, P. Sariigiannidis, and I. Tomkos, "Optimized joint allocation of radio, optical, and MEC resources for the 5G and beyond fronthaul," *IEEE Transactions on Network and Service Management*, July 2021.
- [27] I. A. Alimi, A. L. Teixeira, and P. P. Monteiro, "Toward an efficient C-RAN optical fronthaul for the future networks: A tutorial on technologies, requirements, challenges, and solutions," *IEEE Communications Surveys & Tutorials*, vol. 20, no. 1, pp. 708–769, 2017.
- [28] J. Zhang, Y. Ji, H. Yu, X. Huang, and H. Li, "Experimental demonstration of fronthaul flexibility for enhanced CoMP service in 5G radio and optical access networks," *Optics express*, vol. 25, no. 18, pp. 21 247–21 258, 2017.
- [29] O. Gerstel, M. Jinno, A. Lord, and S. B. Yoo, "Elastic optical networking: A new dawn for the optical layer?" *IEEE communications Magazine*, vol. 50, no. 2, pp. s12–s20, 2012.
- [30] R. Hui, *Introduction to fiber-optic communications*. Academic Press, 2019.
- [31] NTT DOCOMO, "R3-162102: CU-DU split: Refinement for Annex A," 3GPP.
- [32] C. Desset, B. Debaillie, V. Giannini, A. Fehske, G. Auer, H. Holtkamp, W. Wajda, D. Sabella, F. Richter, M. J. Gonzalez *et al.*, "Flexible power modeling of LTE base stations," in *IEEE wireless communications and networking conference (WCNC)*. IEEE, 2012, pp. 2858–2862.
- [33] D. Szczesny, A. Showk, S. Hessel, A. Bilgic, U. Hildebrand, and V. Frascolla, "Performance analysis of LTE protocol processing on an ARM based mobile platform," in *International Symposium on System-on-Chip*. IEEE, 2009, pp. 056–063.
- [34] J. L. Vizcaíno, Y. Ye, and I. T. Monroy, "Energy efficiency analysis for flexible-grid OFDM-based optical networks," *Computer Networks*, vol. 56, no. 10, pp. 2400–2419, 2012.
- [35] M. J. Neely, "Stochastic network optimization with application to communication and queueing systems," *Synthesis Lectures on Communication Networks*, vol. 3, no. 1, 2010.
- [36] M. Hadi and E. Agrell, "Joint power-efficient traffic shaping and service provisioning for metro elastic optical networks," *IEEE/OSA Journal of Optical Communications and Networking*, vol. 11, no. 12, pp. 578–587, 2019.
- [37] M. Hadi, M. R. Pakravan, and E. Agrell, "Dynamic resource allocation in metro elastic optical networks using Lyapunov drift optimization," *Journal of Optical Communications and Networking*, vol. 11, no. 6, pp. 250–259, 2019.
- [38] S. M. Ross, *Introduction to probability models*. Academic press, 2014.
- [39] I. Chih-Lin, J. Huang, R. Duan, C. Cui, J. Jiang, and L. Li, "Recent progress on C-RAN centralization and cloudification," *IEEE Access*, vol. 2, pp. 1030–1039, 2014.
- [40] B. M. Khorsandi and C. Raffaelli, "BBU location algorithms for survivable 5G C-RAN over WDM," *Computer Networks*, vol. 144, pp. 53–63, 2018.
- [41] J. Zou, A. Magee, M. Eiselt, A. Straw, T. Edwards, P. Wright, and A. Lord, "Demonstration of X-haul architecture for 5G over converged SDN fiber network," in *Optical Fiber Communication Conference*. Optical Society of America, 2018, pp. W2A–29.
- [42] "Huawei and China Unicom in First National Commercial Deployment of Full-Outdoor WDM 4G C-RAN Mobile Fronthaul Network," <https://www.huawei.com/ch-en/news/2016/2/full-outdoor-wdm-4g-c-ran>, accessed: 2021-11-04.



Faezeh Samimi Vajd received the B.Sc. degree in electrical engineering from Amirkabir University in 2019, and the M.Sc. degree in communication systems from Sharif University, in 2021. She is currently a Ph.D. candidate in the department of electrical engineering at Amirkabir University. Her current research interests include resource management and service provisioning for optical and radio networks using machine learning and optimization techniques.



Mohammad Hadi received the Ph.D. degree in electrical engineering in 2018 from Sharif University of Technology, Tehran. He was with the Chalmers University of Technology as a postdoctoral researcher in 2019. Since 2021, he has been an Assistant Professor in Communication Systems at Sharif University of Technology. His main research focus is resource allocation in optical and radio networks.



Chayan Bhar received the Ph.D. degree in optical networks in 2018 from the Indian Institute of Technology Kharagpur, India. From 2018 to 2019, he was a Postdoctoral Researcher with the Chalmers University of Technology, Sweden. In 2020, he joined the department of Electronics and Communication Engineering, National Institute of Technology Warangal, India, where he is an Assistant Professor in Communication Networks.



Mohammad Reza Pakravan (M'89) received his B.Sc. degree from University of Tehran (UT), Tehran, Iran, in 1990 with honor and M.Sc. and Ph.D. degrees from University of Ottawa, Canada, in 1992 and 2000, respectively, all in Electrical Engineering. He joined Department of Electrical Engineering at Sharif University of Technology in 2001 where he is currently an associate professor. He is the director of Data Networks Research Laboratory and the director of networking group in the Advanced Communication Research Institute. His research interests include optical communication systems and networks, wireless communication networks and data networking algorithms and protocols. Dr. Pakravan has received many awards for his academic and engineering achievements. Some of the notable awards are IEEE Neal Shepherd memorial best propagation paper award from IEEE vehicular technology society in 2001, two International Khwarizmi awards in 2014 and 2019 from Iranian Research Organization for Science and Technology and Entrepreneurship award of the year from IEEE Iran Section in 2020. He has also been recognized as top engineer of the year by the Iranian Academy of Science in 2018 for his outstanding contributions to development of Electrical and Computer Engineering.



Erik Agrell received the Ph.D. degree in information theory in 1997 from Chalmers University of Technology, Sweden. From 1997 to 1999, he was a Postdoctoral Researcher with the University of California, San Diego and the University of Illinois at Urbana-Champaign. In 1999, he joined the faculty of Chalmers University of Technology, where he is a Professor in Communication Systems since 2009. In 2010, he cofounded the Fiber-Optic Communications Research Center (FORCE) at Chalmers, where he leads the Electrical Engineering research area. He

was a Visiting Professor at University College London in 2014–2017 and is a Collaborating Scientist at the Max Planck Institute for Gravitational Physics, Germany, since 2021. His research interests belong to the fields of information theory, coding theory, and digital communications, and his favorite applications are found in optical communications. Prof. Agrell served as Publications Editor for the IEEE Transactions on Information Theory from 1999 to 2002 and as Associate Editor for the IEEE Transactions on Communications from 2012 to 2015. Since 2020, he is a member of the Board of Governors of the IEEE Information Theory Society. He is a recipient of the 1990 John Ericsson Medal, the 2009 ITW Best Poster Award, the 2011 GlobeCom Best Paper Award, the 2013 CTW Best Poster Award, the 2013 Chalmers Supervisor of the Year Award, the 2015 JLT Best Paper Award, and the 2020 Chalmers Open Access Award.